

pubs.acs.org/JPCL Letter

Structural Flexibility of Proteins Dramatically Alters Membrane Stability—A Novel Aspect of Lipid—Protein Interaction

Rajendra P Giri, Mrinmay K Mukhopadhyay,* Milan K Sanyal, Dipayan Bose, Abhijit Chakrabarti, Peiyu Quan, Wei Bu, and Binhua Lin



Cite This: J. Phys. Chem. Lett. 2022, 13, 11430-11437



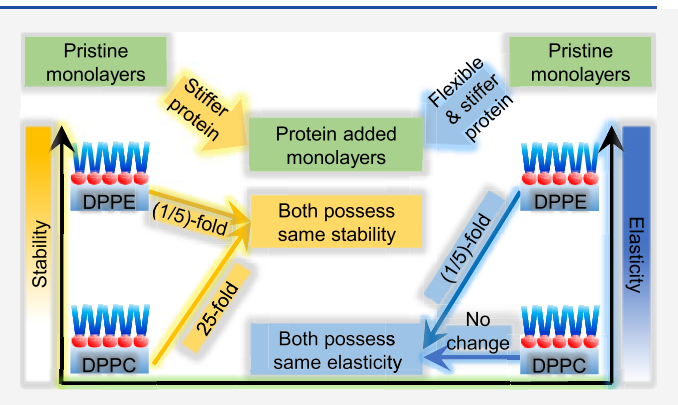
ACCESS I

Metrics & More

Article Recommendations

Supporting Information

ABSTRACT: Protein isoforms are structural variants with changes in the overall flexibility predominantly at the tertiary level. For membrane associated proteins, such structural flexibility or rigidity affects membrane stability by playing modulatory roles in lipidprotein interaction. Herein, we investigate the protein chain flexibility mediated changes in the mechanistic behavior of phospholipid model membranes in the presence of two wellknown isoforms, erythroid (ER) and nonerythroid (NER) spectrin. We show dramatic alterations of membrane elasticity and stability induced by spectrin in the Langmuir monolayers of phosphatidylocholine (PC) and phosphatidylethanolamine (PE) by a combination of isobaric relaxation, surface pressure—area isotherm, X-ray scattering, and microscopy measurements. The NER spectrin



drives all monolayers to possess an approximately equal stability, and that required 25-fold increase and 5-fold decrease of stability in PC and PE monolayers, respectively. The untilting transition of the PC membrane in the presence of NER spectrin observed in Xray measurements can explain better membrane packing and stability.

nomalous protein folding-unfolding and cell membrane stiffness provoke several neurodegenerative and cardiovascular diseases such as Alexander and Huntington's disease and diastolic heart failure. 1,2 Extreme level of membrane stiffness may cause lipid, protein and DNA damage and eventually may lead to cell death. However, both flexibility and stiffness play regulatory roles at the physiological level.^{3–6} In this context, elastic actin-based spectrin filament, a peripheral membrane protein (PMP), is of particular interest as it forms a cytoskeleton network to provide shape and stability to both erythrocyte (ER) and nonerythrocyte (NER) membranes. It regulates cell signaling and serves as a drug target in pharmaceutical industries. 12,13 Malfunctioning of PMPs, especially spectrin, leads to neuropathogenesis and hereditary defects.¹⁴ Protein folding and unfolding processes have farreaching biological consequences embracing cell trafficking, molecular recognition, and also diseases such as amyloidoses, cancer, and tumor where protein structural flexibility plays a crucial role. 15,16 Structural and conformational flexibility of proteins has been reported to be directly linked to the physiological structure-function relationship in cells. 17-19

ER and NER spectrins preferably form dimer and tetramer, 9,20,21 respectively, and possess differential flexibility due to nonidentical coupling between their α and β subunits. NER spectrin is approximately 15-fold rigid with ~ 10 °C higher unfolding transition and hence stronger thermal stability compared to its flexible ER homologue.²⁴

Grum et al. (1999) explained the difference by two structural models: conformational rearrangement and bending.²⁰ Despite its prevalence, the role of protein flexibility on membrane structure has been overlooked in the past decades. Mostly, the stronger lipid-protein interactions were probed by crystallography and imaging techniques.²⁷⁻³⁰ However, our understanding of the weak interactions but crucial to cell functioning such as self-assembly, adsorption-desorption, and intercalation remains limited. In this context, X-ray reflectivity (XRR), grazing incidence diffraction (GID), and thermodynamic measurements provide an invaluable probe for studying the molecular structure and hence lipid-protein interactions with in-depth molecular details.

In this article, we report the protein flexibility driven alterations in structural and mechanical properties of phospholipid Langmuir monolayers (LMs). Phospholipid LMs have long been employed as model biomimetic membranes for investigating lipid-protein and membraneforeign molecule interactions since they provide great controls

Received: September 28, 2022 Accepted: November 29, 2022 Published: December 5, 2022





over the film composition, the surface packing, and straightforward sample preparation methods $^{31-35}$ The LMs of phosphatidylcholine (PC) and phosphatidylethanolamine (PE) lipids having different elasticities have been employed to provide the mechanistic insights into the protein-induced membrane stability. Flexible ER spectrin and relatively stiffer NER spectrin have been used to study their different interactions with the phospholipid LMs using XRR, GID, pressure—area $(\pi - A)$ isotherms, Brewster's angle microscopy (BAM), and isobaric relaxation measurements. Both X-ray and relaxation measurements reveal the striking increase in the stability of the PC membrane on interaction with the stiffer NER spectrin. On the contrary, both ER and NER spectrin have been observed to reduce the elasticity of resilient PE membrane to a value comparable to that of PC membranes with and without spectrin. In order to make the spectrininduced changes more sensitive at the air-water interface we have elucidated the immersion depth of lipid molecules by remarking the interface horizon from GID and Bragg rod analysis. Their subsequent alterations induced by ER and NER spectrin present in the water subphase have also been evaluated. GID data suggest that NER spectrin effectively reduces lipid chain tilting of a PC membrane compared to the ER spectrin. The PE membrane shows a reduced tilting in the presence of the ER spectrin and untilted or undistorted hexagonal structure³² in the presence of the NER spectrin, respectively. XRR data suggest a significant reduction in the air-water interface roughness in both monolayers in the presence of NER spectrin. This untilting transition of the lipids in the presence of NER spectrins may lead to better membrane packing or organization of the lipids and hence better stability of the PC membrane. In the case of PE, the stability of the membrane is more governed by the configuration of the spectrin molecule attachment with the PE headgroup. This indepth structural investigation may benefit the pharmaceutical industry for drug engineering for resisting cell invasion of virus and bacteria.

MATERIALS AND METHODS

1,2-Dipalmitoyl-sn-glycero-3-phosphocholine (DPPC) and 1,2dipalmitoyl-sn-glycero-3-phosphoethanolamine (DPPE) lipids were purchased from Sigma-Aldrich, USA. ER and NER spectrins were extracted from the ovine (sheep) blood and brain, respectively, following the protocol published elsewhere^{21,36,37} and also detailed in the Supporting Information (SI) section. The Langmuir monolayers (LMs) of the lipids were prepared by spreading their chloroform solution in a KSV-NIMA Langmuir-Blodgett (LB) trough at the air-water interface (18 M Ω , pH 6.5). Protein was added in the water subphase prior to spreading the film, and the π -A isotherm and isobaric area relaxation at 30 mN/m were measured at 23 °C. Protein added monolayers are abbreviated as PC-ER and PC-NER for ER and NER spectrin associated DPPC LM and likewise for DPPE. XRR and GID measurements were performed from LMs at the Sector 15, NSF's ChemMatCARS beamline³⁸ at APS using an X-ray wavelength of 1.24 Å to elucidate the out-of-plane and in-plane structures and their subsequent changes induced by ER and NER spectrin. The Langmuir trough used in the X-ray measurements was equipped with an enclosure fitted with a small flow of watersaturated helium to reduce water evaporation from the LB trough and also to suppress the air scattering. Background subtracted XRR profiles were corrected for the capillary wave

contribution from the pristine air—water interface and normalized by Fresnel reflectivity to enhance the present features. 39,40 The processed data were fitted by adapting a two-slab model ("head" and "tail") using Parratt's recursive formalism to evaluate electron density profiles (EDPs) along the surface normal. The background corrected 2d images obtained from the GID measurements were integrated along the q_z axis to obtain the diffraction peaks and plotted against q_{xy} . Similarly, the Bragg rod profiles were obtained by integrating the detector intensity along the q_{xy} and plotted against q_z . The details of experimental procedures and analysis can be found in the SI section.

Noninvasive high resolution XRR and GID techniques were used for the structural characterization of the LMs at the air—water interface. ARR provides an out-of-plane structure of the film, whereas GID provides in-plane lattice structure of lipid assembly. Figure 1 shows the GID profiles and their

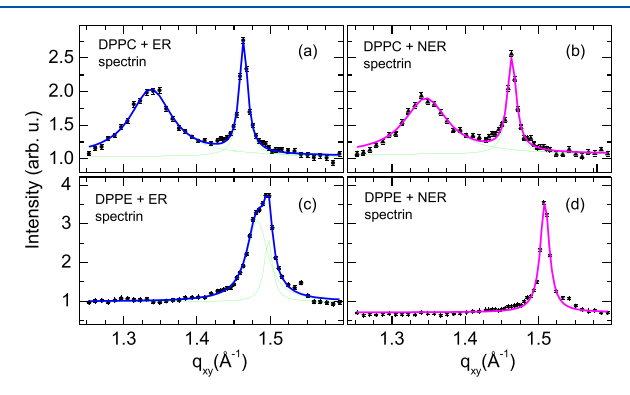


Figure 1. GID profiles and their fits corresponding to the DPPC and DPPE LMs at 30~mN/m with the ER and NER spectrins in the subphase.

Lorentzian fits obtained from the DPPC and DPPE monolayers at 30 mN/m with ER and NER spectrin in the subphase. Bragg rod profiles (BRPs) along with the Vineyard function³² fits shown in Figure 2 and Figure S3 were fitted to

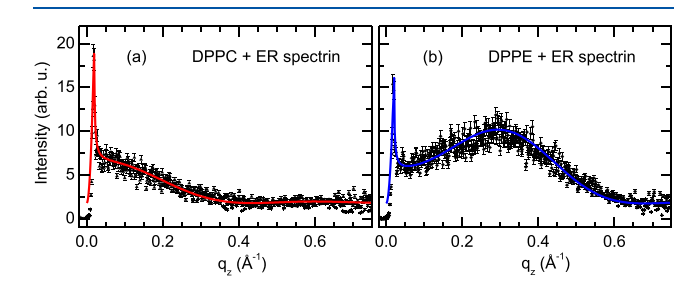


Figure 2. Bragg rod profiles and their fits with Vineyard function obtained from the (a) DPPC and (b) DPPE LMs at 30 mN/m with the ER spectrins in the subphase.

extract lipid tail thickness $(d_{\rm tail})$, tilt angle (θ) , and tilt direction. $^{44-46}$ The fit parameters are listed in Table S1. They suggest that both ER and NER associated DPPC monolayers form a distorted hexagonal unit cell structure with arms $a \neq b$. $\sim 0.2\%$ increase in a and 0.5% decrease in b were evident from the NER added DPPC monolayer compared to the ER added one. θ was also reduced by 1°. However, in the case of DPPE monolayer in the presence of NER spectrin both a and b were shrunk by $\sim 2.1\%$ and 1.1%, respectively, compared to its ER homologue, to form an untilted hexagonal structure with a=b.

A striking difference in θ from the distorted hexagon ($\theta=8.5^\circ$) in the PE-ER monolayer to the undistorted hexagon ($\theta=0^\circ$) in the PE-NER monolayer was also observed. GID and Bragg rod data obtained from the pristine DPPC monolayer were used to define the position of the air—water interface, and that information has been used in the EDP from the XRR. The detailed procedure is explained in the SI section. This in turn helped us to evaluate the immersion depth of PC and PE molecules in water and their subsequent changes in the presence of ER and NER spectrin.

Fresnel normalized XRR profiles and corresponding EDPs from DPPC monolayers at 30 mN/m with ER and NER spectrin in the subphase are shown in Figure 3a and 3b,

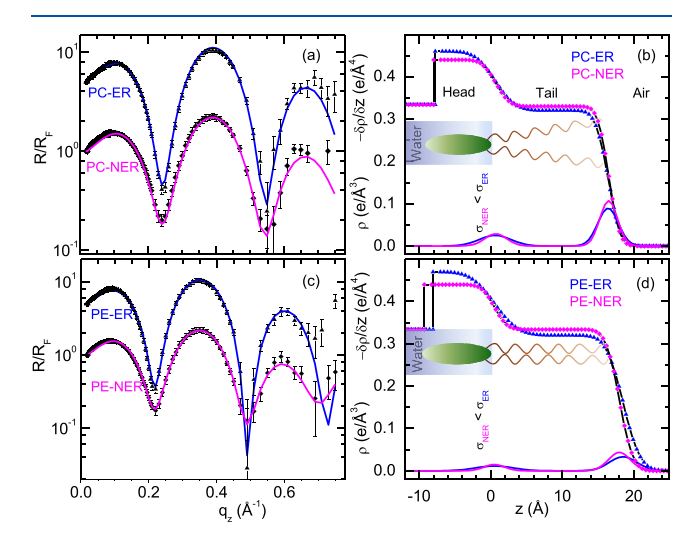


Figure 3. XRR profiles normalized by the Fresnel reflectivity obtained from (a) the DPPC monolayer with ER and NER spectrins in the subphase at 30 mN/m surface pressure. (b) Corresponding EDPs obtained from the fits along with the $\delta\rho/\delta z$ vs thickness (z) to show the variations at different interfaces of the LMs. (c) The XRR profiles normalized by the Fresnel reflectivity obtained from the DPPE monolayer with ER and NER spectrin in the subphase at 30 mN/m surface pressure. (d) Corresponding EDPs and the $\delta\rho/\delta z$ vs thickness (z) obtained from the fits at 30 mN/m. XRR profiles are shifted vertically for better clarity. A constant factor has been multiplied with the $\delta\rho/\delta z$ curves for clear visualization.

respectively. The solid lines each consisting of two peaks in Figure 3b represent the differential EDP $(\delta \rho/\delta z)$ to manifest the enhanced feature of the individual interface roughness and the subsequent changes induced by spectrin. The layer parameters obtained from the XRR fits at 30 mN/m are tabulated in Table S2. Results obtained at 15 mN/m are shown in Figure S1, and the spectrin induced structural changes are discussed in the SI. At 30 mN/m, ER and NER spectrin show exactly the same amount of thickening (2.6%) of the d_{tail} of DPPC LM whereas a thickening of PC headgroup (d_{head}) by ~4% in the presence of the NER spectrin compared to the ER spectrin was observed. EDPs evidence the PC-NER monolayer to possess lower roughness of both the air-tail and tail-water interfaces compared to PC-ER monolayer. This also indicates a significant suppression of thermal capillary wave of air-water interface in the presence of the PC-NER monolayer. Figure 3c and 3d show the Fresnel normalized XRR and EDPs obtained from the DPPE monolayers. Table S2 suggests ~3% contraction of d_{tail} and ~14% thickening of d_{head} in the PE-NER monolayer than that in the PE-ER. Similar to the PC-

NER monolayer, the PE-NER monolayer also possesses lower interface roughness than PE-ER monolayer. XRR results obtained from the PE-ER and PE-NER LMs at 15 mN/m are shown in Figure S2 and discussed in the SI.

Isobaric relaxation data from DPPC and DPPE monolayers at 30 mN/m are shown in Figure 4 panels a and b, respectively,

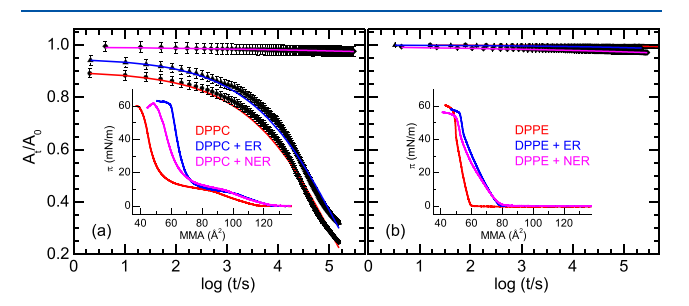


Figure 4. Monolayer relaxation at constant surface pressure of 30 mN/m in (a) DPPC and (b) DPPE monolayers. DPPC monolayer with ER and NER spectrin have been shifted vertically by 0.1 for better clarity. The solid lines are the fit with eq 2. Insets show the pressure—area isotherms from pristine monolayers (red), ER (blue), and NER (magenta) spectrin added monolayers.

in terms of fractional area vs time. The details of data processing are described in the SI. Inset shows the corresponding π -A isotherm data. Figure S10 represents the isothermal cycles obtained from both the monolayers. Monolayer stability has been evaluated from the inverse of the percentage of molecular loss from the monolayer relaxation curves shown in Figure S7. 47,48 Although the PC-ER monolayer follows relaxation kinetics similar to the pristine PC monolayer a strikingly elevated stability is observed in the presence of NER spectrin. The isotherm however does not indicate such a difference except in the condensed phase where MMA is less in the PC-NER monolayer compared to that in the PC-ER. This suggests a relatively higher packing density in the presence of NER spectrin. On the contrary, PE monolayer itself possesses extremely higher stability than the PC monolayer, and the stability is reduced in the presence of spectrin with the highest change observed for PE-NER LM. Comparison of the stability also interestingly suggests that NER spectrin associated PC and PE monolayers possess approximately similar stability. In addition, excess MMA $(\Delta MMA_{exc} = MMA_{pristine} - MMA_{spectrin})$ shown in Figure S4 suggests a π dependent transient behavior of protein adsorption and desorption mechanisms for DPPC and DPPE with positive and negative slopes, respectively. A π_{onset} of 15 \pm 1 mN/m is observed for both ER and NER spectrin associated DPPC monolayers up to which the spectrin uptake is significant and saturation is evident afterward. Thus, the optimum spectrin induced effects are visible at around $\pi_{
m onset}$. However, XRR and GID measurements have been carried out at the physiologically relevant π of 30 mN/m. Structural data obtained at π_{onset} of 15 mN/m from both DPPC and DPPE LMs are discussed in the SI.

A molecular rearrangement and loss mechanism has been adapted by considering dissolution, evaporation, nucleation, and growth phenomena to explain the observed relaxation behavior. A generalized form of kinetic molecular loss can be expressed as follows. A7,50,51

$$\ln \frac{A_t}{A_0} = -K_1 t - K_2 t^2 - K_3 t^{1/2} - K_4 t \tag{1}$$

 K_1 , K_2 , K_3 , K_4 are, respectively, the rate constants of the nucleation, growth, dissolution, and evaporation. A_0 is MMA at time t=0 when the monolayer reaches target π of 30 mN/m and A_t is MMA at time t. Equation 1 can be simplified as

$$\ln \frac{A_t}{A_0} = -Kt^{\nu} \tag{2}$$

where K is the rate constant and ν is the corresponding exponent. 50,51 The contribution from evaporation can be neglected as the measurement was performed close to room temperature. The fits are shown by solid lines in Figure 4a and 4b. Best fits to all the PC monolayer data indicate $\nu \simeq 1$ suggesting the nucleation and growth of PC molecules as the major mode of molecular rearrangement and subsequent loss. The same ν value for PC-ER and PC-NER LMs suggests a similar relaxation mechanism. In addition, it also reveals that the NER spectrin only provides the stability to the PC monolayer without altering the PC-PC interaction mechanism in the membrane. The mechanistic model predicted for such nucleation and growth mechanism was first developed by Smith et al.⁵² It was limited only to the early stage of relaxation which was later generalized by adapting a nucleation-growth collision theory by Vollhardt et al. \$3-56 However, it was also unable to explain the $\nu \simeq 1$ behavior of the relaxation process which was correctly delineated by Wagner et al.⁵⁷ The exponent $\nu \simeq 1$ also indicates in agreement to the previous report⁵⁰ that the PC monolayer follows an instantaneous type of nucleation. Nevertheless, the best fits of relaxation data obtained from pristine PE and PE-ER monolayers indicate $\nu \simeq$ 0.5 suggesting the molecular dissolution in the water subphase as the major route in both the monolayers. For the PE-NER monolayer the fit suggests $\nu \simeq 0.24$ for which the molecular mechanism is unknown. This could be attributed to a complex route of relaxation driven by incommensurate interaction between stiff NER spectrin and a highly elastic PE membrane. The difference in the exponent and hence relaxation mechanisms of PC and PE monolayer may arise from their differential binding affinity with spectrin. 58-61

In-plane elasticity, which is the inverse of compressibility (C_s) , has been calculated from the π –A isotherms using the formula 62

$$C_s^{-1} = -A \left(\frac{\mathrm{d}\pi}{dA} \right)_T \tag{3}$$

for all the monolayers as shown in Figure S6. In contrast to that of the PC-ER monolayer, the elasticity of the PC-NER closely resembles that of the pristine DPPC monolayer. The maximum in elasticity for PC-NER and the pristine DPPC monolayer has appeared at ~41 \pm 2 mN/m, whereas this peak appears at ~47 \pm 2 mN/m for the PC-NER monolayer. 63 The peak in the elasticity curve for all the monolayers represents the condensed phase of the monolayer. 62 The peak maximum has increased from 220 \pm 10 N/m in the pristine LM 62 to 350 \pm 10 N/m (~1.5-fold) in the PC-ER LM. A dip in elasticity, which corresponds to the liquid expanded (LE) to liquid condensed (LC) phase transition, appears at 9.3 \pm 0.5 mN/m in PC-ER, whereas the pristine DPPC and PC-NER monolayer show the dip at slightly higher π of 11 \pm 0.5 mN/m. 62 This is also evident from the compressibility coefficient for all PC LMs

which indicates that the phase transition in PC-ER LM occurs at relatively lower surface pressure compared to the pristine and PC-NER LMs. This lowering in transition surface pressure induced by the ER spectrin can be attributed to overall condensation of the monolayer. In the case of the pristine DPPE monolayer, the peak height of elasticity at 990 N/m⁶³ has reduced approximately by a factor of 5 in both PE-ER and PE-NER LMs possessing an almost similar value of elasticity as observed in all PC LMs associated with and without spectrin. The spectrin-induced changes in elasticity of the monolayers seem to depend strongly on the monolayer phase and the surface packing. The maximum changes were observed at the monolayer condensed phase, i.e., at higher surface pressure. These changes in elasticity also can be explained in terms of the surface packing in the monolayer. The fitting of the XRR profiles at 15 and 30 mN/m (as listed in the Table S2) indicate that the changes in the hydrophobic tail thickness due to spectrin attachment from that in pristine lipid LMs are 2 to 5fold higher at 15 mN/m compared to 30 mN/m for both PC and PE LMs. Thus, the surface packing of the lipids in the presence of spectrins in the membrane plays a big role in controlling the elasticity of the membranes.

Membrane stiffness is the resistance offered by the membrane to the deformation. Structural and conformational flexibility of protein provides stability to the physiological membrane.⁶⁴ Mutual interaction between membrane stiffness and protein structural flexibility is of utmost importance for proper functioning of a cell. Isoforms ER and NER spectrin possess a very similar microstructure but differ in their chain flexibility by about 15-fold. 21,23,26,65 Being in the brain, NER spectrin exerts higher rigidity²⁴ compared to its ER counterpart which provides flexibility to the arteries and blood cells for the smooth flow of blood. 66,67 The comparison between the pristine DPPC and DPPE monolayer structures (Table S2) at 30 mN/m suggests that the PC headgroup is ~5.3% bigger. This difference in headgroup size has caused ~16% reduction in hydrophobic tail thickness in PC than PE. In addition, the in-plane structural parameters (Table S1) obtained from GID data indicates a ~3-fold higher tilt angle of the lipid chains in the PC monolayer compared to that in PE. This structural difference is closely related to the differential elasticity and stability possessed by the PC and PE monolayers. 68 Figure S6 panels a and b suggest that PE possesses ~2-fold higher elasticity than PC at 30 mN/m. The difference is a maximum of ~5-fold at the condensed phase (at ~45 mN/m) of the respective monolayers. Table S3 shows that pristine PC monolayer possesses a molecular loss of 72.1% compared to 0.6% in the case of the pristine PE monolayer in the same time window, which indicates that the PE monolayer is having ~125-fold higher stability than that of the PC monolayer.

Our GID and Bragg rod results suggest that DPPC molecules form a distorted centered hexagonal lattice at the air—water interface at 30 mN/m even in the presence of ER and NER spectrin. The lattice dimension and tilt angle are less in the PC-NER monolayer than in the PC-ER suggesting a preferred adsorption and condensing effect of NER spectrin in DPPC matrix. This is attributed to a commensurate interaction of a stiffer protein chain with flexible membrane. We have defined the location of the air—water interface from the GID and Bragg rod data and later used the information in the electron density profile as described in the SI. Further characterization of out-of-plane structure by XRR suggests a significant reduction in electron density contrast between lipid

head and tail in the presence of NER spectrin compared to ER. It indicates spectrin (coil of ~200 nm) adsorbs into the lipid tail region leaving behind a significant portion in the headgroup and water subphase. The area mismatch between DPPC head and tail leaves tiny hydrophobic pockets in the tail region and helps the spectrin chain to sneak into the membrane.⁶⁸ Interestingly, this spectrin induced small change in membrane structure exhibits a striking difference in stability and phase behavior. Although ER and NER spectrin does not change the overall relaxation mechanism of pristine DPPC membrane, NER spectrin reduces the rate constant of molecular rearrangement and loss remarkably. Nucleation being the primary source of molecular rearrangement and loss in the PC monolayer it should decrease with increasing intermolecular separation which is consistent with our relaxation data at 30 mN/m (Figure 4a and Figure S7) and at 15 mN/m (inset of Figure S7a) and also with previous reports.⁵³ NER spectrin being structurally rigid it slows down the nucleation of the lipid molecules and hence the loss by \sim 25-fold at 30 mN/m. Spectrin adsorption mechanism can be better realized from π -A isotherm data (inset of Figure 4a). Δ MMA_{exc} (Figure S4) calculated from the π -A isotherm has been plotted to show the enhanced feature of spectrin adsorption. It shows a gradual increase in MMA with π indicating continuous spectrin insertion into the DPPC monolayer and filling up of PC adsorption sites of spectrin up to π_{onset} . In the case of NER spectrin, beyond π_{onset} the hydrophobic pockets inside the monolayer are maximally occupied, and no space is available for further spectrin adsorption, eventually leading to saturation. The PC-ER monolayer however adsorbs a little amount of spectrin beyond π_{onset} due to higher conformational flexibility of ER spectrin. A significant mismatch between the MMA calculated from GID and π -A isotherm data at 30 mN/m was observed (Table S3). This can be attributed to the 2D network-type domain formation verified by BAM images (Figure S9). The isotherm measures the average area covered by the lipid molecules in the monolayer. However, GID probes the ordered domains to provide the crystalline structure formed by the lipids. Due to having no-ordered structure in between the domains, GID is only sensitive to the lipid molecules present in the ordered domains. We have calculated the monolayer coverage from the MMA obtained from the GID and π -A isotherm data by the formula ML_{cov} (%) = $MMA_{GID}/MMA_{isotherm} \times 100$ which suggests a coverage of 91% for PC-ER and 98% for the PC-NER monolayer.

GID and Bragg rod results from the PE-ER monolayer at 30 mN/m indicate a distorted centered hexagonal structure similar to PC at the air-water interface. The PE-NER monolayer, on the contrary, forms an undistorted centered hexagon with negligible tilt in the lipid tail indicated by GID data consisting of one single peak. A contraction of lattice dimension by \sim 2% is also evident from the position of the GID peaks. This demonstrates the efficiency of the rigid NER spectrin in altering rotational conformation of lipid molecules in the membrane. XRR data from DPPE monolayers evidence that the NER spectrin preferably lies in the PE headgroup region inducing higher thickness and lower electron density in the head which is opposite to that observed with the ER spectrin. Although ER and NER spectrin show an astonishing alteration in the PE membrane structure, no significant influence in relaxation and phase behavior was observed. Both spectrins have managed to reduce the monolayer

elasticity (Figure S6) and slightly increase the rate of molecular rearrangement and subsequent loss. ΔMMA_{exc} curves (Figure S4) obtained from PE membranes suggest a higher adsorption of spectrin at lower π and a transient desorption with further compression. The smaller size of the PE headgroup makes it comparable to the area covered by tails in the condensed phase leaving a very limited space for foreign spectrin molecules. Due to the betterment of head-tail commensurability over compression the spectrin molecules are eventually squeezed out from the tail region leaving a little residue in the monolayer at 30 mN/m. Hence, the alteration of thermodynamic properties such as monolayer stability and ΔMMA_{exc} is also smaller. Dissolution of DPPE lipids being the primary mode of molecular rearrangement and loss, the spectrin induced headtail incommensurability alters the monolayer stability only slightly (0.6-2.4%). ER spectrin, being more flexible, still holds the intermolecular coordination resulting in a slight reduction in material loss compared to its NER homologue. The monolayer coverage of 80% was observed for both ER and NER spectrin associated monolayers which is substantially lower than that for the pristine PE monolayer with 92% coverage. This difference is consistent with the fact that spectrin possesses PE binding sites at the self-associating domain known as the actin binding domain. 69 The presence of spectrin drives the PE molecules toward the binding domains leaving a notable portion of spectrin uncovered at the airwater interface. The higher stability and hence integrity are more resilient to invasion of an exogenous molecule, 48,0 our study with spectrin molecules indicated that spectrin is more likely to invade the membrane only in its fluid phase where the membrane integrity is significantly lower. Spectrin is observed to invade and alter the mechanical properties of DPPC membrane more effectively compared to those of DPPE as pristine PE membrane is a 5-fold higher elastic than PC (Figure S6).

In summary, the protein chain structural flexibility mediated differential lipid-protein interaction has been comprehended through high resolution X-ray scattering and thermodynamic and microscopy measurements. Model Langmuir monolayers of DPPC and DPPE with lower and higher (~5-fold) elasticity respectively have been employed to study their interaction with flexible ER spectrin and rigid NER spectrin. NER spectrin induces an insignificant structural change in the DPPC membrane and monolayer stability, although it introduces a striking enhancement in the PC monolayer stability. An intriguingly opposite scenario has been observed in the case of the DPPE membrane with a notable reduction in monolayer elasticity in the presence of both ER and NER spectrin isoforms. Nucleation and dissolution of lipid molecules have been found to be the primary modes of molecular rearrangement and their subsequent loss for DPPC and DPPE membranes, respectively. Although ER and NER spectrins do not change the overall rearrangement and loss mechanism they strongly alter the monolayer stability. Preferred interaction between the flexible DPPC membrane and stiffer NER spectrin leads to this extremely stable mechanical property observed here. Since pristine DPPE membrane is highly elastic, the alteration of monolayer stability induced by ER and NER spectrin is less. Lipid head-tail commensurability mediated continual spectrin adsorption in DPPC, and desorption in DPPE upon compression explains the observed changes in monolayer structure and phase behavior. Our study precisely suggests that the membranes with higher stability and integrity

are more resilient to the invasion of exogenous molecules, such as virus and bacteria, in the cell. These findings could also be of potential use in biomedical applications for drug designing and treatment of neurodegenerative and cardiovascular diseases. However, flexibility and rigidity being dynamic phenomena, time-resolved studies would provide a better molecular etiology of self-assembly and lipid—protein interaction.

ASSOCIATED CONTENT

Supporting Information

The Supporting Information is available free of charge at https://pubs.acs.org/doi/10.1021/acs.jpclett.2c02971.

ER and NER spectrin extraction; X-ray scattering measurement methods and data analysis protocol; additional XRR and GID data with fits; Langmuir monolayer isotherm and isobaric relaxation measurement details; Brewster's Angle Microscopy and isotherm cycle data from Langmuir monolayers; Table S1, GID and Bragg rod fit parameters; Table S2, XRR fit parameters; Table S3, monolayer isotherm parameters (PDF)

Transparent Peer Review report available (PDF)

AUTHOR INFORMATION

Corresponding Author

Mrinmay K Mukhopadhyay — Saha Institute of Nuclear Physics, A CI of Homi Bhabha National Institute, Kolkata 700064 West Bengal, India; orcid.org/0000-0001-8050-8661; Email: mrinmay.mukhopadhyay@saha.ac.in

Authors

Rajendra P Giri — Saha Institute of Nuclear Physics, A CI of Homi Bhabha National Institute, Kolkata 700064 West Bengal, India; Institute for Experimental and Applied Physics, Kiel University, 24118 Kiel, Germany; orcid.org/0000-0002-3791-0513

Milan K Sanyal — Saha Institute of Nuclear Physics, A CI of Homi Bhabha National Institute, Kolkata 700064 West Bengal, India; o orcid.org/0000-0002-3847-8793

Dipayan Bose — Saha Institute of Nuclear Physics, A CI of Homi Bhabha National Institute, Kolkata 700064 West Bengal, India

Abhijit Chakrabarti — Saha Institute of Nuclear Physics, A CI of Homi Bhabha National Institute, Kolkata 700064 West Bengal, India; School of Biological Sciences, Ramakrishna Mission Vivekananda Educational & Research Institute, Narendrapur, Kolkata 700103, India

Peiyu Quan − NSF's ChemMatCARS, Pritzker School of Molecular Engineering, The University of Chicago, Chicago, Illinois 60637, United States; ocid.org/0000-0003-3338-5106

Wei Bu — NSF's ChemMatCARS, Pritzker School of Molecular Engineering, The University of Chicago, Chicago, Illinois 60637, United States; ⊚ orcid.org/0000-0002-9996-3733

Binhua Lin — NSF's ChemMatCARS, Pritzker School of Molecular Engineering, The University of Chicago, Chicago, Illinois 60637, United States; □ orcid.org/0000-0001-5932-4905

Complete contact information is available at: https://pubs.acs.org/10.1021/acs.jpclett.2c02971

Notes

The authors declare no competing financial interest.

ACKNOWLEDGMENTS

The authors gratefully acknowledge NSF's ChemMatCARS for X-ray scattering measurements at Sector 15. NSF's ChemMatCARS Sector 15 is supported by the Divisions of Chemistry (CHE) and Materials Research (DMR), National Science Foundation, under grant number NSF/CHE-1834750. Use of the Advanced Photon Source, an Office of Science User Facility operated for the U.S. Department of Energy (DOE) Office of Science, by Argonne National Laboratory, was supported by the U.S. DOE under Contract No. DE-AC02-06CH11357. M.K.M. would like to acknowledge the Department of Science and Technology, GOI, for the financial support for travel provided under the program "Utilization of International Synchrotron Radiation and Neutron Scattering Facilities".

REFERENCES

- (1) Wang, L.; Xia, J.; Li, J.; Hagemann, T. L.; Jones, J. R.; Fraenkel, E.; Weitz, D. A.; Zhang, S.; Messing, A.; Feany, M. B. Tissue and cellular rigidity and mechanosensitive signaling activation in Alexander disease. *Nat. Commun.* **2018**, *9*, 1899.
- (2) Loescher, C. M.; et al. Regulation of titin-based cardiac stiffness by unfoldeddomain oxidation (UnDOx). *Proc. Natl. Acad. Sci. U.S.A.* **2020**, *117*, 24545–24556.
- (3) Weickenmeier, J.; de-Rooij, R.; Budday, S.; Steinmann, P.; Ovaert, T. C.; Kuhl, E. Brain stiffness increases with myelin content. *Acta Biomater* **2016**, *42*, 265–272.
- (4) Chakraborty, M.; et al. Mechanical stiffness controls dendritic cell metabolism and function. *Cell Rep* **2021**, *34*, 108609.
- (5) Wells, R. G. The role of matrix stiffness in regulating cell behavior. *Hepatology* **2008**, 47, 1394–1400.
- (6) Sun, Q.; Hou, Y.; Chu, Z.; Wei, Q. Soft overcomes the hard: Flexible materials adapt to cell adhesion to promote cell mechanotransduction. *Hepatology* **2022**, *10*, 397–404.
- (7) Mitra, M.; Patra, M.; Chakrabarti, A. Fluorescence study of the effect of cholesterol on spectrin-aminophospholipid interactions. *Eur. Biophys. J.* **2015**, *44*, 635–645.
- (8) Diakowski, W.; Sikorski, A. F. Interaction of brain spectrin (fodrin) with phospholipids. Quenching of spectrin intrinsic fluorescence by phospholipid suspensions. *Biochemistry* **1995**, 34, 13252–13258.
- (9) Kusunoki, H.; MacDonald, R. I.; Mondragón, A. Structural insights into the stability and flexibility of unusual erythroid spectrin repeats. *Structure* **2004**, *12*, 645–656.
- (10) Mohandas, N.; Evans, E. Mechanical properties of the red cell membrane in relation to molecular structure and genetic defects. *Annu. Rev. Biophys. Biomol. Struct.* **1994**, 23, 787–818.
- (11) Kahana, E.; Pinder, J. C.; Smith, K. S.; Gratzer, W. B. Fluorescence quenching of spectrin and other red cell membrane cytoskeletal proteins. Relation to hydrophobic binding sites. *Biochem. J.* **1992**, 282, 75–80.
- (12) Overington, J. P.; Al-Lazikani, B.; Hopkins, A. L. How many drug targets are there? *Nat. Rev. Drug Discovery* **2006**, *5*, 993–996.
- (13) Wymann, M.; Schneiter, R. Lipid signalling in disease. *Nat. Rev. Mol. Cell Biol.* **2008**, *9*, 162–176.
- (14) Morrow, J. S.; Stankewich, M. C. The spread of spectrin in Ataxia and neurodegenerative disease. *J. Exp. Neurol.* **2021**, *2*, 131–139.
- (15) Radford, S. E.; Dobson, C. M. From computer simulations to human disease: emerging themes in protein folding. *Cell* **1999**, *97*, 291–298.
- (16) Carlson, H. Protein flexibility and drug design: how to hit a moving target. Curr. Opin. Chem. Biol. 2002, 6, 447–452.

- (17) Spyrakis, F.; BidonChanal, A.; Barril, X.; Luque, F. J. Protein flexibility and ligand recognition: Challenges for molecular modeling. *Curr. Top. Med. Chem.* **2011**, *11*, 192–210.
- (18) Teilum, K.; Olsen, J. G.; Kragelund, B. B. Functional aspects of protein flexibility. *Cell. Mol. Life Sci.* **2009**, *66*, 2231–2247.
- (19) Amaral, M.; Kokh, D. B.; Bomke, J.; Wegener, A.; Buchstaller, H. P.; Eggenweiler, H. M.; Matias, P.; Sirrenberg, C.; Wade, R. C.; Frech, M. Protein conformational flexibility modulates kinetics and thermodynamics of drug binding. *Nat. Commun.* **2017**, *8*, 2276.
- (20) Grum, V. L.; Li, D.; MacDonald, R. I.; Mondragón, A. Structures of two repeats of spectrin suggest models of flexibility. *Cell* **1999**, 98, 523–535.
- (21) Patra, M.; Mukhopadhyay, C.; Chakrabarti, A. Probing conformational stability and dynamics of erythroid and nonerythroid spectrin: Effects of urea and guanidine hydrochloride. *PLoS One* **2015**, *10*, No. e0116991.
- (22) Mitra, M.; Chaudhuri, A.; Patra, M.; Mukhopadhyay, C.; Chakrabarti, A.; Chattopadhyay, A. Organization and dynamics of tryptophan residues in brain spectrin: Novel insight into conformational flexibility. *J. Fluoresc.* **2015**, *25*, 707–717.
- (23) An, X.; Zhang, X.; Salomao, M.; Guo, X.; Yang, Y.; Wu, Y.; Gratzer, W.; Baines, A. J.; Mohandas, N. Thermal Stabilities of Brain Spectrin and the Constituent Repeats of Subunits. *Biochemistry* **2006**, 45, 13670–13676.
- (24) Bennett, V.; Davis, J.; Fowler, W. E. Brain spectrin, a membrane-associated protein related in structure and function to erythrocyte spectrin. *Nature* **1982**, 299, 126–131.
- (25) Sriswasdi, S.; Harper, S. L.; Tang, H. Y.; Gallagher, P. G.; Speicher, D. W. Probing large conformational rearrangements in wild-type and mutant spectrin using structural mass spectrometry. *Proc. Natl. Acad. Sci. U.S.A.* **2014**, *111*, 1801–1806.
- (26) Li, Q.; Fung, L. W. M. Structural and dynamic study of the tetramerization region of non-erythroid α -spectrin: A frayed helix revealed by site-directed spin labeling electron paramagnetic resonance. *Biochemistry* **2009**, *48*, 206–215.
- (27) Loura, L. M. S.; Prieto, M.; Fernandes, F. Quantification of protein-lipid selectivity using FRET. *Eur. Biophys. J.* **2010**, *39*, 565–578.
- (28) Deleu, M.; Crowet, J. M.; Nasir, M. N.; Lins, L. Complementary biophysical tools to investigate lipid specificity in the interaction between bioactive molecules and the plasma membrane: A review. *Biochim. Biophys. Acta. Biomembr.* **2014**, *1838*, 3171–3190.
- (29) Raunser, S.; Walz, T. Electron crystallography as a technique to study the structure on membrane proteins in a lipidic environment. *Annu. Rev. Biophys.* **2009**, *38*, 89–105.
- (30) Barrera, N. P.; Zhou, M.; Robinson, C. V. The role of lipids in defining membrane protein interactions: Insights from mass spectrometry. *Trends Cell Biol.* **2013**, 23, 1–8.
- (31) Stefaniu, C.; Brezesinski, G.; Möhwald, H. Langmuir monolayers as models to study processes at membrane surfaces. *Adv. Colloid Interface Sci.* **2014**, 208, 197–213.
- (32) Kaganer, V. M.; Möhwald, H.; Dutta, P. Structure and phase transitions in Langmuir monolayers. *Rev. Mod. Phys.* **1999**, *71*, 779.
- (33) Broniatowski, M.; Bojarski, J.; Wydro, P. Langmuir monolayers as models of the lipid matrix of cyanobacterial thylakoid membranes. *J. Mol. Liq.* **2022**, 368, 120727.
- (34) Brezesinski, G.; Möhwald, H. Langmuir monolayers to study interactions at model membrane surfaces. *Adv. Colloid Interface Sci.* **2003**, *100*–*102*, 563–584.
- (35) Phan, M. D.; Shin, K. A. Langmuir monolayer: Ideal model membrane to study cell. *J. Chem. Biol. Interfaces* **2014**, *2*, 1–5.
- (36) Bose, D.; Patra, M.; Chakrabarti, A. Effect of pH on conformational staibility, oligomerization and dynamics of erythroid and nonerythroid spectrin. *Biochim. Biophys. Acta Proteins Proteom.* **2017**, *1865*, 694–702.
- (37) Glenney, J R; Glenney, P; Weber, K F-actin binding and cross-linking properties of porcine brain fodrin a spectrin related molecule. *J. Biol. Chem.* **1982**, 257, 9781–9787.

- (38) Schlossman, M. L.; Synal, D.; Guan, Y.; Meron, M.; Sheamccarthy, G.; Huang, Z.; Acero, A.; Williams, S. M.; Rice, S. A.; Viccaro, P. J. A synchrotron X-ray liquid surface spectrometer. *Rev. Sci. Instrum.* **1997**, *68*, 4372–4384.
- (39) Giri, R. P.; Mukhopadhyay, M. K.; Basak, U. K.; Chakrabarti, A.; Sanyal, M. K.; Runge, B.; Murphy, B. M. Continuous uptake or saturation: Investigation of concentration and surface-packing-specific hemin interaction with lipid membranes. *J. Phys. Chem. B* **2018**, *122*, 7547–7554.
- (40) Maiti, S.; Sanyal, M. K.; Mukhopadhyay, M. K.; Singh, A.; Mukherjee, S.; Datta, A.; Fontaine, P. Structural and optical properties of two-dimensional gadolinium stearate Langmuir monolayer. *Chem. Phys. Lett.* **2018**, *712*, 177–183.
- (41) Giri, R. P.; Chakrabarti, A.; Mukhopadhyay, M. K. Cholesterolinduced structural changes in saturated phospholipid model membranes revealed through X-ray scattering technique. *J. Phys. Chem. B* **2017**, *121*, 4081–4090.
- (42) Parratt, L. G. Surface studies of solids by total reflection of X-rays. *Phys. Rev.* **1954**, *95*, 359–369.
- (43) Basu, J. K.; Sanyal, M. K. Ordering and growth of Langmuir-Blodgett films: X-ray scattering studies. *Phys. Rep.* **2002**, 363, 1–84.
- (44) Als-Nielsen, J.; Jacquemain, D.; Kjaer, K.; Leveiller, F.; Lahav, M.; Leiserowitz, L. Principles and applications of grazing incidence X-ray and neutron scattering from ordered molecular monolayers at the air-water interface. *Phys. Rep.* **1994**, *246*, 251–313.
- (45) Majewski, J.; Kuhl, T. L.; Wong, J. Y.; Smith, G. S. X-ray and neutron surface scattering for studying lipid/polymer assemblies at the air—liquid and solid—liquid interfaces. *Rev. Mol. Biotechnol.* **2000**, 74, 207–231.
- (46) Kjaer, K. Some simple ideas on X-ray reflection and grazing-incidence diffraction from thin surfactant films. *Physica B* **1994**, *198*, 100–109.
- (47) Ou-Yang, W.; Weis, M.; Manaka, T.; Iwamoto, M. Study of relaxation process of dipalmitoyl phosphatidylcholine monolayers at air-water interface: Effect of electrostatic energy. *J. Chem. Phys.* **2011**, 134, 154709.
- (48) Basak, U. K.; Datta, A.; Bhattacharyya, D. Stability and softening of a lipid monolayer in the presence of a pain-killer drug. *Colloids Surf.*, B **2015**, *132*, 34–44.
- (49) Monroy, F.; Hilles, H. M.; Ortega, F.; Rubio, R. G. Relaxation dynamics of Langmuir polymer films: A power-law analysis. *Phys. Rev. Lett.* **2003**, *91*, 268302.
- (50) Chou, T. H.; Chang, C. H. Thermodynamic behavior and relaxation processes of mixed DPPC:cholesterol monolayers at the air:water interface. *Colloids Surf. B Biointerfaces* **2000**, *17*, 71–79.
- (51) Nino, M. R. R.; Lucero, A.; Patino, J. M. R. Relaxation phenomena in phospholipid monolayers at the air—water interface. *Colloids Surf. A: Physicochem. Eng. Asp.* **2008**, 320, 260–270.
- (52) Smith, R. D.; Berg, J. C. The collapse of surfactant monolayers at the air—water interface. J. Colloid Interface Sci. 1980, 74, 273–286.
- (53) Vollhardt, D. Nucleation and growth in supersaturated monolayers. *Adv. Colloid Interface Sci.* **1993**, 47, 1–23.
- (54) Vollhardt, D.; Retter, U. Nucleation in insoluble monolayers I: Nucleation and growth model for relaxation of metastable monolayers. *J. Phys. Chem.* **1991**, *95*, 3723–3727.
- (55) Vollhardt, D.; Retter, U.; Siegel, S. Nucleation in insoluble monolayers II: Constant pressure relaxation of octodecanoic acid monolayers. *Thin Solid Films* **1991**, *199*, 189–199.
- (56) Vollhardt, D.; Retter, U. Nucleation in insoluble monolayers. III. Overlapping effect of the growing centers. *Langmuir* **1992**, *8*, 309–312.
- (57) Wagner, J.; Michel, T.; Nitsch, W. Relaxation behavior and bilayer formation of poly(4-vinylpyridinium) type polyelectrolytes at the air/water interface. *Langmuir* **1996**, *12*, 2807–2812.
- (58) Stabach, P.; Morrow, J. S. Identification and characterization of beta V spectrin, a mammalian ortholog of drosophilabeta H spectrin. *J. Biol. Chem.* **2000**, 275, 21385–21395.

- (59) Wolny.; et al. Key amino acid residues of ankyrin-sensitive phosphatidylethanolamine/phosphatidylcholine-lipid binding site of β I-spectrin. *J. Biol. Chem.* **2011**, *6*, No. e21538.
- (60) Kennedy, S. P.; Warren, S. L.; Forget, B. G.; Morrow, J. S. Ankyrin binds to the 15th repetitive unit of erythroid and nonerythroid beta-spectrin. *J. Cell Biol.* **1991**, *115*, 267–277.
- (61) Sarkar, S.; Bose, D.; Giri, R. P.; Mukhopadhyay, M. K.; Chakrabarti, A.Status of Membrane Asymmetry in Erythrocytes: Role of Spectrin. In *Biochemical and Biophysical Roles of Cell Surface Molecules*; Advances in Experimental Medicine and Biology; Chattopadhyay, K.; Basu, S., Eds.; Springer: Singapore, 2018; Vol. 1112, pp 3–11.
- (62) Mandal, P.; Giri, R. P.; Murphy, B. M.; Ghosh, S. Self-assembly of graphene oxide nanoflakes in a lipid monolayer at the air-water interface. ACS Appl. Mater. Interfaces 2021, 13, 57023–57035.
- (63) Zhu, H.; Sun, R.; Hao, C.; Zhang, P. A Langmuir and AFM study on interfacial behavior of binary monolayer of hexadecanol/DPPE at the air-water interface. *Chem. Phys. Lipids* **2016**, 201, 11–20.
- (64) Thirumalai, D.; Klimov, D. K.; Dima, R. I. Emerging ideas on the molecular basis of protein and peptide aggregation. *Curr. Opin. Struct. Biol.* **2003**, *13*, 146–159.
- (65) Sarkar, S.; Bose, D.; Giri, R. P.; Mukhopadhyay, M. K.; Chakrabarti, A. Effects of GM1 on brain spectrin-aminophospholipid interactions. *Biochim. Biophys. Acta* **2019**, *1861*, 298–305.
- (66) Salomao, M.; An, X.; Guo, X.; Gratzer, W.; Mohandas, N.; Baines, A. J. Mammalian R I-spectrin is a neofunctionalized polypeptide adapted to small, highly deformable erythrocytes. *Proc. Natl. Acad. Sci. U.S.A.* **2006**, *103*, 643–648.
- (67) Knowles, W. J.; Morrow, J. S.; Speicher, D. W.; Zarkowsky, H. S.; Mohandas, N.; Mentzer, W. C.; Shohet, S. B.; Marchesi, V. T. Molecular and functional changes in spectrin from patients with hereditary pyropoikilocytosis. *J. Clin. Invest.* **1983**, *71*, 1867–1877.
- (68) Giri, R. P.; Mukhopadhyay, M. K.; Mitra, M.; Chakrabarti, A.; Sanyal, M. K.; Ghosh, S. K.; Bera, S.; Lurio, L. B.; Ma, Y.; Sinha, S. K. Differential adsorption of a membrane skeletal protein, spectrin, in phospholipid membranes. *Europhys. Lett.* **2017**, *118*, 58002.
- (69) Ray, S.; Chakrabarti, A. Membrane interaction of erythroid spectrin: surface-density-dependent high-affinity binding to phosphatidylethanolamine. *Mol. Membr. Biol.* **2004**, *21*, 93–100.